NANO LETTERS

2007
Vol. 7, No. 7
1980−1984

Controlled Formation and Mixing of Two-Dimensional Fluids

Ilja Czolkos,[†] Yavuz Erkan,[†] Paul Dommersnes,[‡] Aldo Jesorka,[†] and Owe Orwar*,[†]

Department of Chemical and Biological Engineering, Chalmers University of Technology, 412 96 Göteborg, Sweden, and MSC, Université Paris Diderot, 10, rue Alice Domon et Léonie Duquet, F-75205 Paris, France

Received March 28, 2007; Revised Manuscript Received May 8, 2007

ABSTRACT

We introduce a novel technique for the controlled spreading and mixing of lipid monolayers from multilamellar precursors on surfaces covered by the hydrophobic epoxy resin SU-8. The lipid spreads as a monolayer as a result of the high surface tension between SU-8 and the aqueous environment. A micropatterned device with SU-8 lanes, injection pads, and mixing regions, surrounded by hydrophilic Au, was constructed to allow handling of lipid films and to achieve their mixing at controlled stoichiometry. Our findings offer a new approach to dynamic surface functionalization and decoration as well as surface-based catalysis and self-assembly.

In the past few years, the successful formation of two-dimensional lipid interfaces has received numerous contributions because of their potentially useful application in, for example, biotechnology and surface science. It has been shown that different types of planar lipid membranes, such as supported lipid bilayers on hydrophilic surfaces,[1−4] polymer-cushioned lipid bilayers,[5,6] and tethered lipid bilayers,[5] could be established for biotechnological or biosensorical exploitation. Furthermore, lipid monolayers could be formed by the traditional Langmiur−Blodget deposition technique[7] or by lipid vesicle adsorption.[8,9] Self-assembled monolayers (SAMs) represent another class of molecularly thin films that, in contrast to lipid or surfactant systems, do not possess properties of a fluid. SAMs, which typically are composed of alkanthiolates or other alkyl compounds on Au, Ag, and Cu[10] are easily formed[11] and have been shown to be very useful for surface modification and functionalization on the micrometer scale.[12−15]

We have developed a concept for controlled formation of liquid films on microfabricated hydrophobic substrates that we call dynamic liquid film formation (DLFF). In contrast to previous methods of fabrication, this method allows for stoichiometric control of the different components included in the film. As hydrophobic substrate, we used SU-8, which is a negative tone photoresist that can vary in hydrophobicity depending on the fabrication procedure.[16] We spin-coated glass coverslips with SU-8, which is ab initio hydrophobic and thereby permits lipid monolayer adsorption. The contact angle of water on SU-8 was determined to be 91.4° ± 1.5°. When multilamellar lipid vesicles suspended in a buffer droplet are placed on the SU-8 substrate, the contained lipid rapidly spreads as a monolayer on the surface. The formed lipid patches are perfectly circular, as shown in Figure 1a. The multilamellar vesicles are eventually entirely depleted and transformed into a lipid monolayer. The tension induced by SU-8 is sufficient to disrupt the structure of the multilamellar vesicle. Therefore, the surface adhesion energy of lipids on SU-8, Σ, is larger than the lysis tension of bilayer membranes $\sigma_L \approx 2-9$ mN/m. The adsorbed lipid basically screens the hydrophobic surface energy between SU-8 and water, and the gain in surface energy associated with lipid adsorption, Σ, is expected to be roughly equal to the surface tension between SU-8 and water. SU-8 is an epoxy, and it is therefore reasonable to assume that the surface tension SU-8/water could be as high as $\sigma_{epoxy} \approx 47$ mN/m.[17] We quantified the dynamics of the lipid spreading process and found that the wetted area A over time is approximately linear at the beginning of the spreading process (see Figure 1a). In refs 18 and 19, the dynamics of spreading was modeled by balancing the lipid film Marangoni stress $\nabla\sigma$ with the sliding friction force between lipid film and surface (per unit area): $\nabla\sigma - \zeta v = 0$. For lipid film spreading on a lane of SU-8, the spreading velocity is $v = \sqrt{\beta/t}$ where $\beta = S/2\zeta$ is the spreading coefficient and the spreading power S is the difference in free energy between lipids on the surface and lipids in the reservoir (per unit area).[19] The lipid film velocity on a lane is uniform over the film,[18,19] whereas for circular spreading, there is a gradient in velocity. For circularly spreading monolayers, we find that the radius of the spreading film is given by $R \log(R/R_0)\, dR/dt = 2\beta$. Taking

* Corresponding Author: E-mail: orwar@chalmers.se. Telephone: +46-31-772-3060. Fax: +46-31-772-6120.
[†] Department of Chemical and Biological Engineering, Chalmers University of Technology.
[‡] MSC, Université Paris Diderot.

10.1021/nl070726u CCC: $37.00
Published on Web 06/06/2007

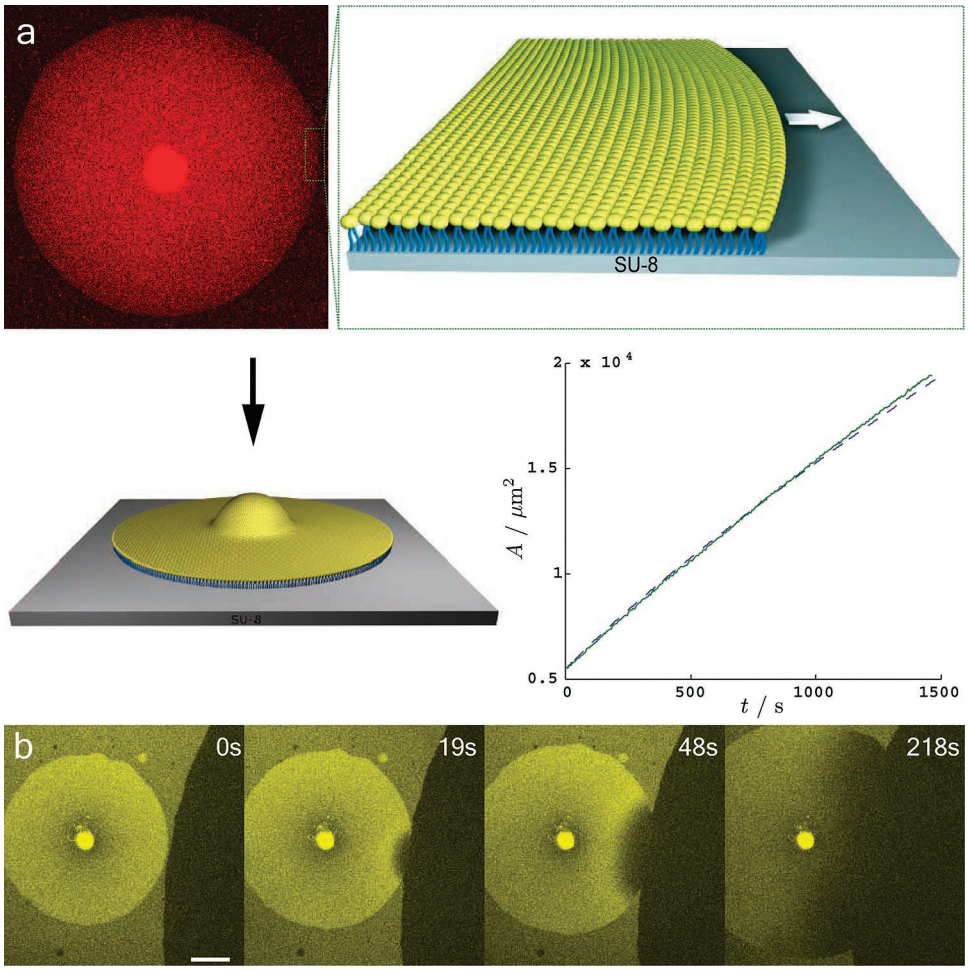

Figure 1. Lipid spreading and mixing. (a) Upper panel: Confocal micrograph of a circular lipid patch stained with rhodamine phosphatidylethanolamine and a schematic of the spreading lipid front. Lower panel: Illustration of a circularly spreading lipid patch and an exemplary plot of the area wetted by a circular lipid patch over time (experimental data, green line; numerical fit, blue dashed line). Recorded from fluorescence micrographs. (b) A soybean polar extract (SPE) lipid patch to the left, stained with FM1-43, mixes with a DOTAP lipid patch to the right. Positively charged DOTAP repels the positively charged dye FM1-43 and thereby, the SPE lipid patch turns dark. Scale bar 30 μm. All fluorescence micrographs were artificially colored.

R_0 equal to the mean radius of the spreading multilamellar vesicle and solving this equation numerically yields a good fit with the experimental data (Figure 1a). The estimated spreading coefficients are in the range $\beta = 1-3\ \mu m^2/s$. The tension at the spreading edge is equal to the lipid/SU-8 adhesion energy $\sigma(R) = \Sigma$. At the multilamellar vesicle, the tension is expected to be equal to the lysis tension of a bilayer membrane $\sigma(R_0) = \sigma_L$, and the spreading power is $S = \Sigma - \sigma_L$. Taking $\Sigma \sim \sigma_L \sim 6$ mN/m and $\beta \approx 3\ \mu m^2/s$, the sliding friction between monolayer and SU-8 is estimated to be of the order $\zeta \sim 10^9$ Pas/m, which is of the same order of magnitude as the sliding friction, $b_m = 0.5 \times 10^9$ Pas/m, between the two sheets in a lipid bilayer membrane.[20] This strongly supports the notion of a lipid monolayer on hydrophobic SU-8, with interactions very similar to the interactions between the sheets in a lipid bilayer membrane.

To demonstrate mixing of lipid films with different composition, we applied a mixture of multilamellar vesicles of soybean polar extract (SPE) lipids and DOTAP (*N*-[1-(2,3-dioleoyloxy)propyl]-*N*,*N*,*N*-trimethylammonium salts) multilamellar vesicles to the SU-8 surface. DOTAP is a synthetic, positively charged lipid, while SPE is a mixture of lipids which are overall negatively charged. Images of the mixing of the two lipid monolayers are shown in Figure 1b. The SPE lipid was stained with the fluorescent dye FM1-43, while DOTAP was unstained. As the mixing proceeds, the fluorescence intensity in the stained SPE lipid patch decreases because the concentration increase in DOTAP leads to the displacement of the stain. If the lipid films would not be mixing, one would obtain a stationary, discrete border in fluorescence intensity between the two films. We form monolayer films where the hydrophobic tails of the lipid molecules are pointing toward the SU-8 surface and the hydrophilic head groups point to the buffer solution (see the illustrations in Figure 1a). To confirm and quantify the mobility of the lipid molecules, we performed fluorescence recovery after photobleaching (FRAP) experiments. The curve obtained from the fluorescence recovery of a bleached circle with known radius was fitted to a modified bessel function according to Axelrod et al. and yielded the "characteristic" diffusion time τ_D.[21] From τ_D, the diffusion constant D was calculated to be $2.3 \times 10^{-1}\ \mu m^2/s$. This is one order of magnitude lower than the diffusion constant reported for supported phospholipid bilayers.[1]

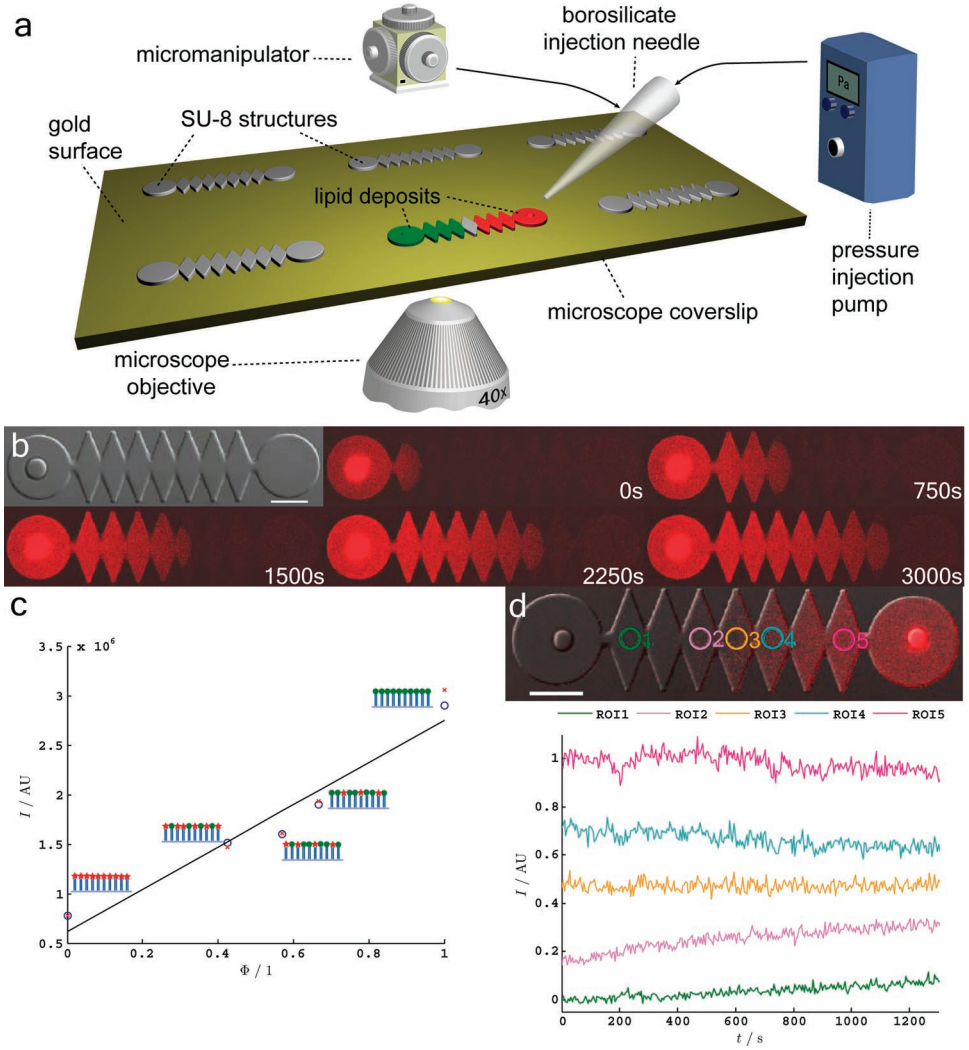

Figure 2. (a) Illustration of the experimental setup at the confocal scanning microscope. Micromanipulators are equipped with microinjection needles to place multilamellar vesicles. The vesicles can be aspirated or expirated by applying negative or positive pressures, respectively. The experiment is proceeded in a drop of aqueous buffer. (b) SU-8 structure and fluorescence micrographs of fluorescently labeled lipid spreading on the structure. Images were modified in contrast and brightness. (c) The integrated fluorescence intensity over a surface structure such as in (b) to which a lipid mixture was applied is plotted vs the mixing ratio Φ. ○ and × represent individual measurements on identical structures. (d) The upper image shows an overlay of a transmission image and a fluorescence micrograph of an SU-8 structure with multilamellar vesicles on the injection pads where the lipid on the right is doped with rhodamine phosphatidylethanolamine. The intensity values from fluorescence micrographs in the marked regions of interest (ROI) are plotted vs time below. Scale bars 30 μm.

We next developed a platform based on a microtransfer technique for deposition of multilamellar vesicles[22] onto patterned substrates with differential hydrophobicity. This platform allows for formation of lipid films with controlled composition. We made SU-8 patterns on Au, which in contrast to SU-8 is hydrophilic and does not promote lipid spreading. Because SU-8 is a photoresist, it offers the opportunity to generate structures on the micrometer scale[23] whose shape we designed to support lipid film formation and controlled stoichiometric mixing. We made binary and ternary mixers having two and three injection pads for multilamellar vesicles, respectively, and one centrally placed mixing region. Figure 2a is a schematic of the experimental setup. The setup gives us the opportunity to control injection of lipid to the injection pads to monitor spreading and mixing and to remove lipid sources with a micropipette again. Figure 2b shows lipid spreading on a structure, where the multilamellar vesicle was placed on the left injection pad and spreads over the surface. We were able to mix lipids stoichiometrically by applying different lipid films in known quantities to the two injection pads on the type of structure shown in Figure 2b. One of the lipid fractions was fluorescent, while the other one was not. We monitored the dilution of the two lipid films in each other and determined the fluorescence intensity at different film mixing ratios Φ, shown in Figure 2c. One can see that the relation is linear ($R^2 = 0.944$), which shows that the system can be calibrated.

Furthermore, the dynamics of lipid monolayer mixing can be followed. Figure 2d shows a mixing device on which two lipid monolayers mix. The fluorescence intensity values from the marked regions are plotted versus time. Obviously, a wide range of lipid mixing ratios can be found on the surface. One can see that, for significant changes in fluorescence intensity to occur, it takes several minutes. On the time scale

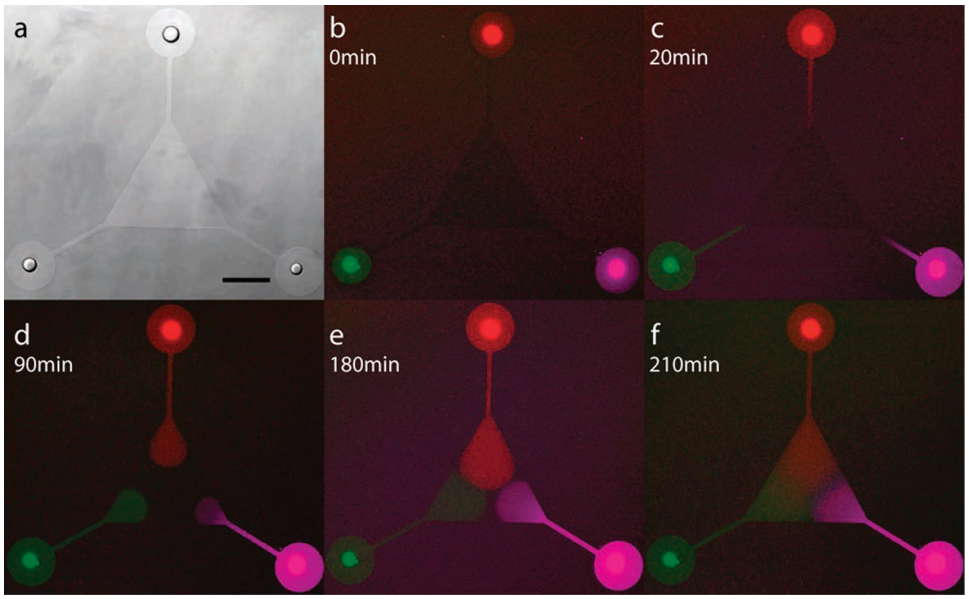

Figure 3. Three-way lipid mixing. Three different lipid fractions were applied to and thereby mixed on a ternary mixing device. The upper vesicle is stained with rhodamine phosphatidylethanolamine (exc 543 nm, em 560−610 nm), the vesicle on the lower left is stained with carboxyfluorescein phosphatidylethanolamine (exc 496 nm, em 500−560 nm), and the vesicle on the lower right is stained with Alexa 633 phosphatidylethanolamine (exc 633 nm, em 640−800 nm). (a) Transmission image of the SU-8 structure and the applied vesicles. (b−f) Time series of lipid mixing. In image (e), the red and the green colored lipid films meet, and in image (f), the magenta colored lipid film meets the other two lipid films. Scale bar 30 μm. All fluorescence micrographs were artificially colored.

of a measurement, the lipid composition in an area in size such as the regions indicated in Figure 2d can be assumed to be constant. First of all, the comparatively low diffusion constant of the lipid makes this type of investigation convenient. Second, the purposeful design of the SU-8 structure, which are rhombs with limited junction size in between them, contributes to decelerated mixing compared to a simple line between the terminal injection pads.

Figure 3 shows a ternary mixing device on which three differently stained multilamellar vesicles have been placed. The spreading lipid monolayers are mixing in the center of the structure. We are furthermore capable of producing structures of higher order for mixing four or more different lipid films. The mixing ratio of the applied lipid fractions can be controlled by timing of application and removal of lipid sources. We measured that the spreading coefficient β of lipid flux on a lane is in the range of 1−5 μm^2/s, independent of the line width w. When the lane is long compared to the lane width, the dissipation due to surfactant flow on the lipid injection pad is negligible compared to the dissipation on the lane and $v_{\text{lane}} = \sqrt{\beta/t}$, where $t = 0$ is the time when the lipid enters the lane from the injection pad. The total flux of lipid over a lane is therefore proportional to the lane width w. This means that the ratio of the widths of two lanes w_A/w_B, leading to the central mixing area of a mixing device equals the mixing ratio Φ between the lipid fractions A and B spreading on these lanes. This shows that we are in principle able to control lipid mixing ratios in the mixed monolayer by geometrical design of the structure.

In this paper, we present the formation of lipid monolayers on SU-8 as a hydrophobic, structured support. We investigated the underlying dynamics and the driving force for the lipid monolayer spreading. Also, we provide fundamental insight into the controlled, stoichiometric mixing of a dynamic surface that is contained at micrometer length scale with the potential to be used at submicrometer length scale as well. This work represents the starting point for the controlled modification of a two-dimensional liquid, and we are therefore convinced that this work will have an impact on research and applications regarding surface functionalization and decoration as well as surface-based catalysis and self-assembly.

Acknowledgment. We thank Candice Coppere for help with the contact angle measurement device. We are grateful for financial support from the European Commission within the sixth framework AMNA project (contract no. 013575), from the Swedish Foundation for Strategic Research within the NanoX project, as well as the Göran Gustafsson Foundation and the Swedish Research Council.

Note Added after ASAP Publication. This paper was published ASAP on June 6, 2007. The caption of Figure 3 was revised. The updated paper was reposted on June 8, 2007.

Supporting Information Available: Video of SPE lipid and DOTAP mixing, as shown in Figure 1b (AVI). Video of lipid spreading on a meander-shaped SU-8 structure (MPEG). The time index is in thousand seconds until $t = 0.999$ and is in seconds from $t = 1000$ on). Methods. this material is available free of charge via the Internet at http://pubs.acs.org.

References

(1) Salafsky, J.; Groves, J. T.; Boxer, S. G. *Biochemistry* **1996**, *35*, 14773−14781.
(2) Muresan, A. S.; Lee, K. Y. C. *J. Phys. Chem. B* **2001**, *105*, 852−855.

(3) Kim, Y.-H.; Rahman, M.; Zhang, Z.-L.; Misawa, N.; Tero, R.; Urisu, T. *Chem. Phys. Lett.* **2006**, *420*, 569−573.
(4) Yoon, T.-Y.; Jeong, C.; Lee, S.-W.; Kim, J. H.; Choi, M. C.; Kim, S.-J.; Kim, M. W.; Lee, S.-D. *Nat. Mater.* **2006**, *5*, 281−285.
(5) Wagner, M. L.; Tamm, L. K. *Biophys. J.* **2000**, *79*, 1400−1414.
(6) Tanaka, M.; Sackmann, E. *Nature* **2005**, *437*, 656−663.
(7) Kalb, E.; Frey, S.; Tamm, L. K. *Biochim. Biophys. Acta* **1992**, *1103*, 307−316.
(8) Mancheño, J. M.; Martín-Benito, J.; Gavilanes, J. G.; Vázquez, L. *Biophys. Chem.* **2006**, *119*, 219−223.
(9) Park, J.-W.; Lee, G. U. *Langmuir* **2006**, *22*, 5057−5063.
(10) Yan, L.; Huck, W. T. S.; Whitesides, G. M. *J. Macromol. Sci. C* **2004**, *44*, 175−206.
(11) Bishop, A. R.; Nuzzo, R. G. *Curr. Opin. Colloid Interface Sci.* **1996**, *1*, 127−136.
(12) Kada, G.; Riener, C. K.; Hinterdorfer, P.; Kienberger, F.; Stoh, C. M.; Gruber, H. J. *Biophys. J.* **2006**, *90*, 1270−1274.
(13) Gardner, T. J.; Frisbie, C. D.; Wrighton, M. S. *J. Am. Chem. Soc.* **1995**, *117*, 6927−6933.
(14) Xu, H.; Hong, R.; Lu, T.; Uzun, O.; Rotello, V. M. *J. Am. Chem. Soc.* **2006**, *128*, 3162−3163.
(15) Kumar, A.; Abbott, N. L.; Kim, E.; Biebuyck, H. A.; Whitesides, G. M. *Acc. Chem. Res.* **1995**, *28*, 219−226.
(16) Nordström, M.; Marie, R.; Calleja, M.; Boisen, A. *J. Micromech. Microeng.* **2004**, *14*, 1614−1617.
(17) Harper, C. A. *Plastics Materials and Processes: A Concise Encyclopedia;* Wiley & Sons: Hoboken, NJ, 2003; p 604.
(18) Rädler, J. O.; Strey, H.; Sackmann, E. *Langmuir* **1995**, *11*, 4539−4548.
(19) Nissen, J.; Gritsch, S.; Wiegand, G.; Rädler, J. O. *Eur. Phys. J. B* **1999**, *10*, 335−344.
(20) Evans, E.; Yeung, A. *Chem. Phys. Lipids* **1994**, *73*, 39−56.
(21) Axelrod, D.; Koppel, D. E.; Schlessinger, J.; Elson, E.; Webb, W. W. *Biophys. J.* **1976**, *16*, 1055−1069.
(22) Karlsson, M.; Nolkrantz, K.; Davidson, M.; Strömberg, A.; Ryttsén, F.; Åkerman, B.; Orwar, O. *Anal. Chem.* **2000**, *72*, 5857−5862.
(23) Zhang, J.; Tan, K. L.; Hong, G. D.; Yang, L. J.; Gong, H. Q. *J. Micromech. Microeng.* **2001**, *11*, 20−26.

NL070726U